

Trimethylamine N -Oxide Electrochemical Biosensor with a Chimeric Enzyme

Biljana Mitrova, Armel Waffo, Paul Kaufmann, Chantal Iobbi-nivol, Silke
Leimkuhler, Ulla Wollenberger

► **To cite this version:**

Biljana Mitrova, Armel Waffo, Paul Kaufmann, Chantal Iobbi-nivol, Silke Leimkuhler, et al..
Trimethylamine N -Oxide Electrochemical Biosensor with a Chimeric Enzyme. *ChemElectroChem*,
Weinheim : Wiley-VCH, 2019, 6 (6), pp.1732-1737. 10.1002/celec.201801422 . hal-02273149

HAL Id: hal-02273149

<https://hal-amu.archives-ouvertes.fr/hal-02273149>

Submitted on 20 Nov 2019

HAL is a multi-disciplinary open access archive for the deposit and dissemination of scientific research documents, whether they are published or not. The documents may come from teaching and research institutions in France or abroad, or from public or private research centers.

L'archive ouverte pluridisciplinaire **HAL**, est destinée au dépôt et à la diffusion de documents scientifiques de niveau recherche, publiés ou non, émanant des établissements d'enseignement et de recherche français ou étrangers, des laboratoires publics ou privés.

Electrochemical biosensor for TMAO detection with a chimeric enzyme

Biljana Mitrova^a, Armel F. T. Waffo^a, Paul Kaufmann^a, Chantal Iobbi-Nivol^b, Silke Leimkühler^a, Ulla Wollenberger^{a*}

^a Institute for Biochemistry and Biology, University of Potsdam, Potsdam 14476, Germany

^b Aix-Marseille Univ., CNRS, BIP, Marseille, France

* Corresponding author : Ulla Wollenberger Address : Karl-Liebnecht-Str. 24, H25, 14476 Golm, Potsdam, Germany; E-mail : uwollen@uni-potsdam.de

Abstract

For the first time, an enzyme-based electrochemical biosensor system for determination of trimethylamine *N*-oxide (TMAO) is described. It employs an active chimeric variant of TorA in combination with an enzymatically deoxygenating system and a low potential mediator for effective regeneration of the enzyme and cathodic current generation. TMAO reductase (TorA) is a molybdoenzyme found in marine and most enterobacteria that catalyzes specifically the reduction of TMAO to trimethylamine (TMA). The chimeric TorA named TorA-FDH corresponds to the apoform of TorA from *Escherichia coli* reconstituted with the molybdenum cofactor from formate dehydrogenase (FDH). Each enzyme, TorA and TorA-FDH, was immobilized on the surface of a carbon electrode and covered with a dialysis membrane. The biosensor operates at an applied potential of -0.8 V (vs. Ag/AgCl (1M KCl)) under ambient air conditions thanks to an additional enzymatic O₂-scavenger system. A comparison between the two enzymes revealed a much higher sensitivity for the biosensor with immobilized TorA-FDH. The biosensor exhibits a sensitivity of 14.16 nA/μM TMAO in a useful measuring range of 2 -110 μM with a detection limit of LOD = 2.96 nM (n = 3), almost similar for TMAO in buffer and in spiked serum samples. With a response time of 16 ± 2 s the biosensor is stable over prolonged daily measurements (n=20). This electrochemical biosensor provides suitable applications in detecting TMAO levels in human serum.

Keywords: Trimethylamine *N*-oxide (TMAO), TMAO reductase, chimeric enzyme, molybdoenzyme, electrochemical biosensor

1. Introduction

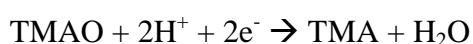
Trimethylamine *N*-oxide (TMAO) is an organic end-product originating from the degradation of dietary trimethylamine containing compounds like choline, carnitine and lecithin (Velasquez et al., 2016). After ingestion of food rich in these compounds the gut microbiota degrades them to trimethylamine (TMA), which is further transferred to the liver where the flavin dependent monooxygenase (FMO) family of enzymes converts it to TMAO. This TMAO is mostly excreted through urine (Fennema et al., 2016). In recent years this molecule has emerged as a potential biomarker for several disease states. Clinical reports have pointed to the involvement of TMAO in the development of atherosclerosis (Bennett et al., 2013) and its correlation to the development and progression of cardiovascular diseases (Wang et al., 2011). A link between high levels of TMAO in the plasma and the increased risk of developing colorectal cancer among postmenopausal women was also found (Bae et al., 2014). Given the main clearance of TMAO from the body is through urine (Smith et al., 1994), increased negative effects have also been reported in patients with chronic kidney disease (Bell et al., 1991; Stubbs et al., 2016).

Even though the emerging importance of the TMAO as a biomarker has been recognized there is yet no specific method for the detection of this molecule that could be used quickly outside the laboratory. Most of the reported methods in literature are analytical approaches that first need the reduction of TMAO to TMA (daCosta et al., 1990) or some other preparation methods that involve organic toxic solvents and labeling. In some cases, an additional derivatization of the TMA is also needed in order to get an estimate of the TMAO levels. Methods like ion or liquid chromatography and nuclear magnetic resonance (NMR) were mostly used in the developed procedures for determining the TMAO levels (Bell et al., 1991; Mamer et al., 2010; Wang et al., 2014). Apart from the reported unspecific microbial biosensor (Gamati et al., 1991) a specific electrochemical biosensor approach, to our knowledge, is not yet developed.

Most of the biosensors available on the market are based on oxidases and operate at positive potentials. In contrast, the use of reductase reactions usually requires potentials where dissolved oxygen interferes and therefore, it has to be removed beforehand. The combination of glucose oxidase and catalase is well established for deoxygenation of solutions for various analytical approaches (Benesch and Benesch, 1953; Cheng et al., 2003; Englander et al., 1987). This approach was elaborated in great detail by Plumeré et al. for oxygen tolerant

biosensing of nitrate (Plumeré et al., 2012). Previously, an amperometric DMSO biosensor on the basis of DMSO reductase, a highly homologous enzyme to TMAO reductase was reported where application of glucose oxidase and catalase enabled measurements of DMSO in ambient air conditions (Abo et al., 2003).

Trimethylamine *N*-oxide reductase, TorA, from *Escherichia coli* is a mononuclear molybdenum containing enzyme which specifically catalyzes the reduction of TMAO to TMA in the reaction (Buc et al., 1999):



It can also catalyze other *N*-oxide compounds, like 4-methyl morpholine *N*-oxide as an example of another prominent substrates (Iobbi-Nivol et al., 1996). Among the reported substrates, TMAO and morpholine *N*-oxide have the highest affinity for TMAO reductase and are catalyzed also with the highest efficiency. Recently, Kaufmann et al. reported the reconstitution of an active TMAO reductase from the apoform of the enzyme (apo-TorA) with the cofactor from *Rhodobacter capsulatus* formate dehydrogenase (FDH). Direct and mediated electrochemistry established that high electrocatalytic activities were achieved when the enzyme was either expressed and purified under anaerobic conditions (referred to as TorA-WT) or reconstituted with the FDH cofactor ligating a terminal sulfido ligand at the molybdenum atom (referred to as TorA-FDH) (Kaufmann et al., 2018).

Here, we report the first electrochemical TMAO biosensor. The sensor is based on TMAO reduction by immobilized TorA-FDH in combination with an enzymatically deoxygenation system and a low potential mediator for effective regeneration of the engineered enzyme. All of the measurements were performed with the chimeric enzyme TorA-FDH that is exhibiting high catalytic activity. A comparison between TorA-FDH or TorA-WT biosensor demonstrates that TorA-WT is less efficient than the chimeric enzyme TorA-FDH. Given the higher signals obtained with mediated electrochemistry compared to direct electrochemistry, we chose the first one for the development of the TMAO biosensor. The glucose oxidase/catalase system ensured an O₂ insensitive detection of TMAO by the biosensor at ambient air condition.

2. Experimental

2.1. Chemicals

Didodecyldimethylammonium bromide (DDAB) (98%), trimethylamine *N*-oxide dihydrate and methyl viologen (MV) were all purchased from Sigma-Aldrich. Tris(hydroxymethyl)aminomethane (TRIS) from Duchefa Biochemie B.V., potassiumhydrogenphosphate and glucose were purchased from Merck. SeronormTM Human was from SERO AS, Norway and the cellulose membrane (MWCO 9kDa) was obtained from BST Biosensor Technology, Berlin. Glucose oxidase (GOx) (Type II ≥ 15000 U/g) and Catalase (Cat, from bovine liver) (2000-5000 U/mg) were purchased from Sigma. The two TMAO reductases used are TorA-FDH (228 U/mg; k_{cat} 360 s⁻¹) and TorA-WT (593 U/mg; k_{cat} 934 s⁻¹). All the other used reagents were of lab grade purity and used without further purification.

2.2. Apparatus and procedures

The electrochemical experiments were carried out in a lab-made three-electrode cell with a total volume of 1 mL, employing a platinum wire as counter electrode, an Ag/AgCl (1 M KCl) reference electrode (Microelectrodes Inc., Bedford, USA) against which all potentials are reported. Cyclic voltammetry (CV) was performed with a modified graphite rod working electrode (Alfa Aesar, Karlsruhe, Germany). A glassy carbon electrode (BAS) was employed as the working electrode in all amperometric measurements for the development of the biosensor. All electrochemical experiments were performed at room temperature using PalmSens potentiostat and analyzed with PSLite 4.8 software (Palmsens, The Netherlands) and OriginPro 2017. The CV experiments were performed in a glovebox (COY, USA) at room temperature and under anaerobic conditions (minimum of 2% H₂ and 98% N₂).

In CV, the potential on the working electrode was cycled between -0.2 V and -0.8 V for the direct bioelectrocatalysis and between -0.3 V and -0.9 V for the mediated bioelectrocatalysis, all at 5 mV/s scan rate and stirred solution. In amperometry, the potential applied on the working electrode was held at constant value of -0.8 V.

The biosensor characterization was performed under ambient air conditions using 8 U GOx and 200 U Cat of final activity together with 50 mM glucose to insure O₂ removal from the measuring cell. A lid on top of the cell was placed to limit the O₂ dissolving into the measuring buffer during the measurement.

2.3. *Electrode modification*

2.3.1. CV measurements

Prior to modification the graphite rod electrode with diameter of 3.5 mm was cleaned by polishing with emery paper with two different grit sizes (200 and 1500) and then ultrasonicated in Milli-Q water for 20 s and dried under N₂ stream. The electrode modification was carried out based on a published procedure (Aguey-Zinsou et al., 2002). Briefly the cleaned electrode was modified with a mixture of 1:1 volume ratio of 2 mM DDAB and 265 μM TorA-FDH. A 6 μL of this mixture was drop casted onto the electrode surface and left to dry in a desiccator at 4 °C for 15-20 min. The modified electrode was then transferred into the anaerobic glovebox and used for the voltammetric experiments. The same procedure was applied for the mediated and direct electrochemistry.

2.3.2. Biosensor

A glassy carbon electrode was cleaned with two different grain size Al₂O₃, 1 μm and 0.3 μm respectively, then ultrasonicated in Milli-Q water for 10 min, washed thoroughly and dried under N₂ stream. The electrode modification was performed by drop casting 5 μL of enzyme (TorA-FDH or TorA-WT) and drying in a desiccator at 4 °C for 30 min. Afterwards the electrode was covered with a dialysis membrane and fastened in the cell with an O-ring assembly. All biosensor measurements were performed under standard lab condition in air and at room temperature.

2.4. *Protein purification and reconstitution*

The purification of *E. coli* TorA, apo-TorA and the reconstitution of apo-TorA with the cofactor of *R. capsulatus* formate dehydrogenase were performed as described in Kaufmann et al. (Kaufmann et al., 2018).

3. Results and discussion

3.1. Direct versus mediated bioelectrocatalysis

In a recent study, we reported on the direct electrocatalytic reaction of TorA and the in vitro reconstituted chimera of this enzyme in order to indicate the role of the first coordination sphere of the cofactor on its potential and its activity (Kaufmann et al., 2018). TorA-FDH was among the most active enzyme variants. Fig 1A is depicting the CV of the direct bioelectrocatalysis of TMAO by the immobilized TorA-FDH. After addition of 3 mM TMAO as substrate (black trace) a clear evolution of a biocatalytic reduction current can be seen. From the first derivative of the reduction part of the bioelectrocatalytic curve the catalytic potential $E_{cat} = -0.56$ V is determined (SI Fig 1). The catalytic potential (E_{cat}) is described as the maximum of the first derivative (dI/dE) or the inflection point where the bioelectrocatalytic current plateaus on both sides (Fourmond et al., 2013). This potential should be close to the redox potential of the center where catalysis takes place or/and to the redox potential of the center which is a limiting factor during the electron transfer event (Zu et al., 2003). Given that TMAO reductase carries only the redox center bis-MGD, we can ascribe the measured catalytic potential to represent a close value of the potential of the redox active center. Then, a similar experiment was conducted except that a mediator was added (Fig 1B). Methyl viologen was selected mostly because of its negative redox potential ($E^\circ = -0.446$ V vs. NHE (i.e., $= -0.645$ V vs. Ag/AgCl (1 M KCl)) (Michaelis and Hill, 1933). As shown in Fig 1b, the addition of TMAO in the presence of methyl viologen leads to a strong current increase. Indeed, the bioelectrocatalytic current is more than 80 times higher than in the unmediated bioelectrocatalysis. The efficiency of the electron transfer is obviously much higher in the presence of mediator. In mediated electrochemistry, the molecules which are not in direct contact with the electrode also contribute to the total biocatalytic current output. This makes the use of a mediator a much more desirable approach for the construction of biosensors where small concentrations of substrates should be detected.

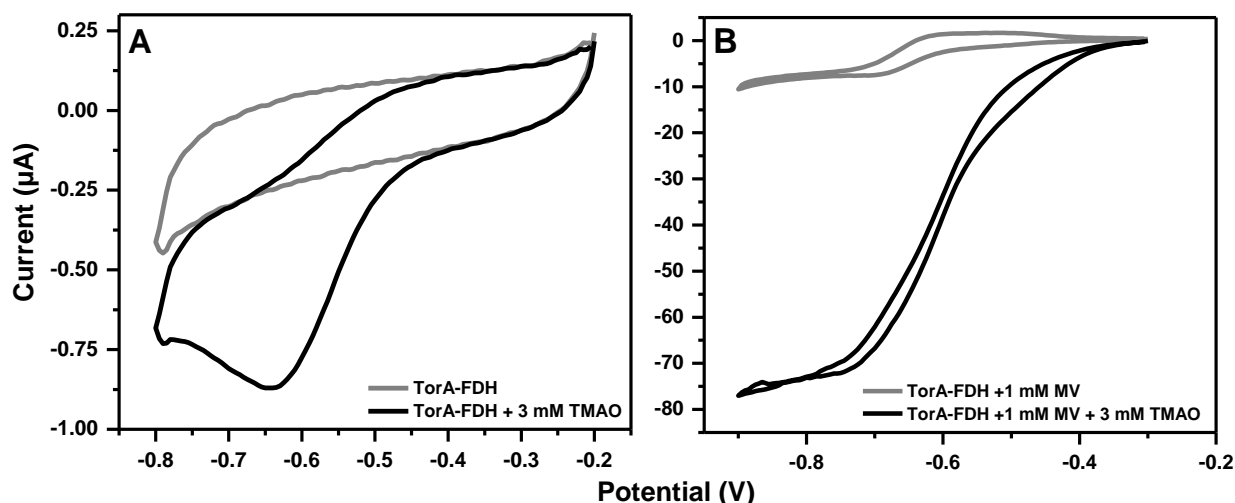


Figure 1. A) Direct and B) mediated bioelectrocatalysis of TMAO by immobilized TorA-FDH. CV of the immobilized TorA-FDH electrode before (grey trace) and after (black trace) addition of 3 mM TMAO, recorded A) without and B) in the presence of 1 mM methyl viologen. Please note the different current ranges. Other conditions: Anaerobic, potassium phosphate buffer 10 mM pH 6.5; scan rate: 5 mV/s.

3.2. Biosensor

The previous voltammetric experiments were conducted in a glovebox in order to prevent the interferences coming from oxygen. The biosensor is intended to be applicable under standard, environmental conditions (in ambient air) in the lab. Therefore, the buffer solution was enzymatically deoxygenated during the measurements and glassy carbon was used instead of graphite. Graphite is very porous and could not completely be deoxygenated. TorA-FDH was immobilized onto a glassy carbon electrode by adsorption and trapped under a permselective membrane. The biosensor was evaluated using amperometry. When the electrode is polarized at -0.8 V a rapid evolution of a catalytic reduction current is seen after TMAO addition to a buffer containing MV as soluble mediator (Fig. 2). Fig. 2 shows the typical steady state response curve and the schematic of the reaction sequence of the biosensor. A small peak appears immediately after the injection of TMAO, which vanishes within seconds and can be explained by disturbances from the sample injection, while a large stationary reduction current evolves. TMAO is reduced to TMA with concomitant oxidation of the enzyme. The reducing equivalents are delivered by $MV^{+\bullet}$, which is regenerated at the electrode. As a result, a catalytic current is generated proportional to TMAO concentration. No significant reduction current appeared when the enzyme was not immobilized on the electrode surface.

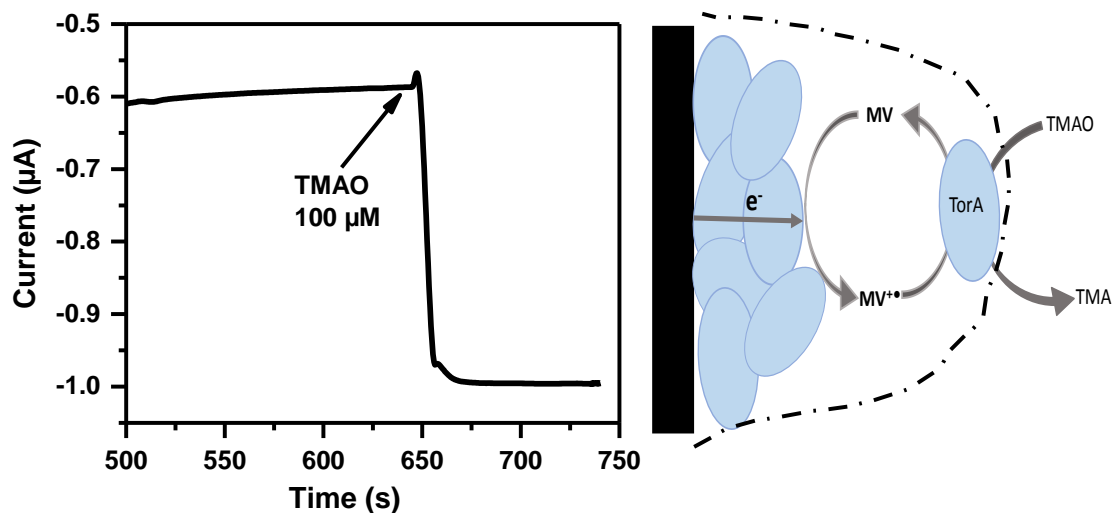


Figure 2. Amperometric curve of mediated reduction of 100 μM TMAO by immobilized TorA-FDH (left). On the right is a scheme representing the immobilized enzyme and the reaction with TMAO and the recycling of methyl viologen on the electrode surface. Potassium phosphate buffer 100 mM pH 6.5; Eappl -0.8 V; 8 U GOx, 200 U Cat and 50 mM glucose; 250 μM methyl viologen

Methyl viologen is a suitable mediator. In order to determine the optimum conditions for the biosensor the concentration of MV was varied between 50 nM and 1 mM and the sensor response for 100 μM TMAO was evaluated. Even very low concentrations of mediator gave a response after addition of substrate. As can be seen on SI Fig 2, the enzyme has a high affinity for the mediator ($K_m^{\text{app}} = 0.36 \pm 0.1 \mu\text{M}$). The published K_m for methyl viologen is 150 μM (Nihon Seikagakkai, et al., 1986). The lower value here is due to the cyclic regeneration of the mediator on the electrode surface. The current reached a saturation value at 250 μM , above which no further current increase was measurable. This was reminiscent of what was observed for the DMSO biosensor. Indeed, Abo et al. reported low concentrations of MV, (5 or 50 μM) depending on the needed sensitivity for the detection of DMSO (Abo et al., 2003). To guarantee no mediator limitation for all further measurements of TMAO, we used 250 μM of MV.

The amount of enzyme used for immobilization was additionally varied. Increase of the enzyme amount (and thus the enzyme activity) led to a growth of sensor sensitivity until a maximum indicating that the sensor response changed from kinetic to diffusion limitation. Fig. 3 represents the results of the loading test. Remarkably, the maximum response for TMAO is already reached at very low amount of TorA-FDH (7,07 pmol/cm^2) (Fig. 3). Due to the higher enzymatic activity of TorA-FDH, its loading is much lower compared to other described enzyme electrodes in which an enzyme is adsorbed on electrode surfaces (Schulz et al., 2014; Tavahodi et al., 2017). However, a tenfold reduction of the applied amount resulted

in a clear drop of response. In order to have sufficient excess of enzyme and the highest response for further studies, we applied 5.9 nmol/cm^2 . Enzyme excess typically secures stability and longer measuring range.

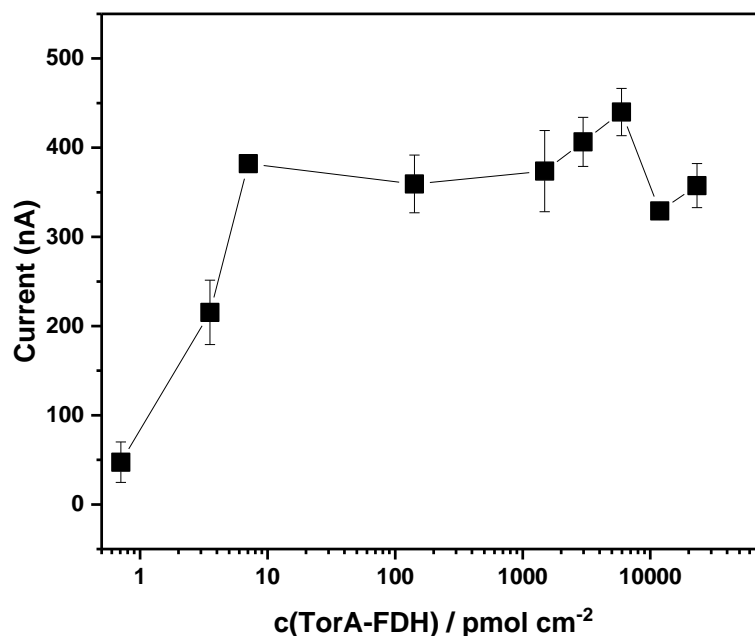


Figure 3. Enzyme loading dependence. Graph of the measured amperometric current versus the electrode applied TorA-FDH concentration. Potassium phosphate buffer 100 mM pH 6.5; TMAO 100 μM ; Methyl viologen 250 μM ; GOx 8 U, Cat 200 U and glucose 50 mM. (n=3 electrodes)

3.3. Comparison between TorA-FDH and TorA-WT

In our previous work, we showed that the current increase at 3 mM TMAO in the presence of 1 mM MV was nearly the same for TorA-FDH and TorA-WT (81.99 ± 8.53 and 83.16 ± 3.5 μA , respectively), indicating that TorA-FDH and TorA-WT are comparably active (Kaufmann et al., 2018). Here, we compared the response of the immobilized TorA-WT and TorA-FDH under the newly defined conditions. From Fig. 4, it is obvious that now the enzyme response is not similar. In the presence of 100 μM of TMAO, TorA-WT is less efficient than TorA-FDH (323 ± 81 nA vs. 440 ± 26 nA, respectively). The current response for the TorA WT-modified electrode for 2 μM TMAO is also visibly decreased to 19.3 ± 15 nA, which is almost half of that of the TorA-FDH modified electrode (28.3 ± 1 nA).

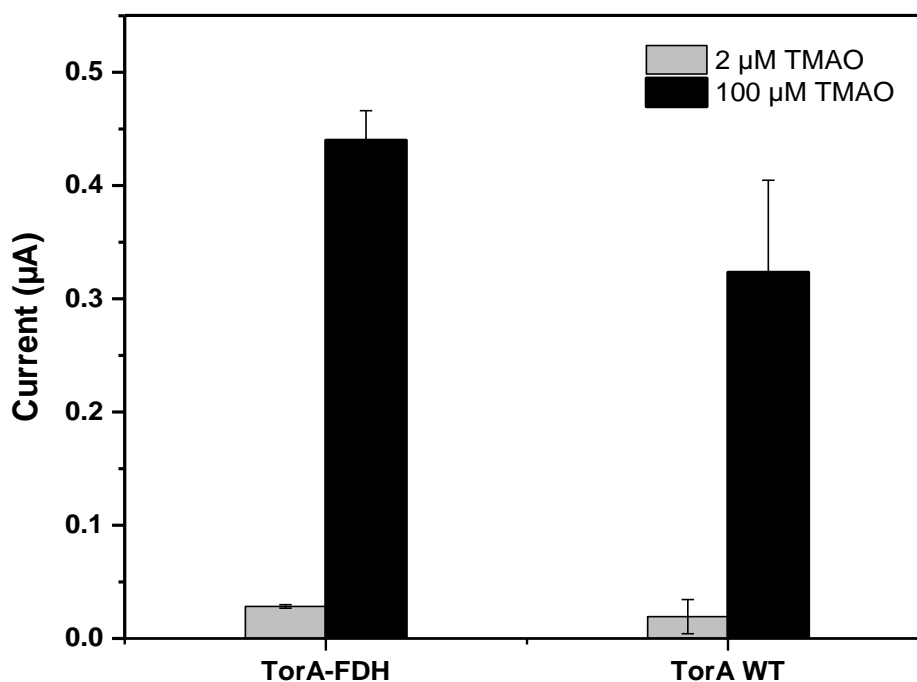


Figure 4. Comparison between the activity of TorA-FDH and TorA-WT. Potassium phosphate buffer 100 mM pH 6.5; TMAO 100 µM; Methyl viologen 250 µM; GOx 8 U, Cat 200 U and glucose 50 mM; Eappl -0.8 V (n=3 electrodes).

Furthermore, the response of the TorA WT sensor is less reproducible between sensor preparations. The larger variation between the sensors can be explained by differences in the sensitivity to oxygen since the TorA WT was expressed and purified under anaerobic conditions. It was already reported that a contact of the WT enzyme with oxygen can damage the cofactor and as a result lower the activity of the enzyme (Kaufmann et al., 2018).

Since the TorA-FDH variant seems to be less susceptible to oxidative damage compared to the WT enzyme it was selected for the construction of the biosensor for TMAO detection.

3.4. Biosensor performance

The biosensor was thus constructed with TorA-FDH immobilized on the electrode surface (5.9 nmol/cm^2) and addition of MV (250 µM). As shown by the above results, this biosensor can be used even in the presence of oxygen since the chimeric TorA-FDH enzyme remains stable. The performances of the biosensor were then tested.

Fig 5A shows the dependence of the amperometric current on TMAO concentration. The useful measuring range is from 2 to 110 µM TMAO but the range of linearity is much longer (~10 mM TMAO) (SI Fig 3). The response time is $16 \pm 2 \text{ s}$ and the sensitivity is $14.16 \text{ nA}/\mu\text{M}$ TMAO with a limit of detection of $\text{LOD} = 2.96 \text{ nM}$ ($S/N \text{ } n = 3$). The reported values of TMAO concentrations in the human blood plasma of a healthy person are between 2.25 – 5.79

μM for both man and woman (Kühn et al., 2017; Wang et al., 2014). Higher values of around $100 \mu\text{M}$ TMAO were reported mostly for patients with chronic kidney disease but also associated with other disease states (Mafra et al., 2014; Stubbs et al., 2016; Zhu et al., 2016). As can be seen from the graph (Fig 5A) the linear range is in the total range of our interest.

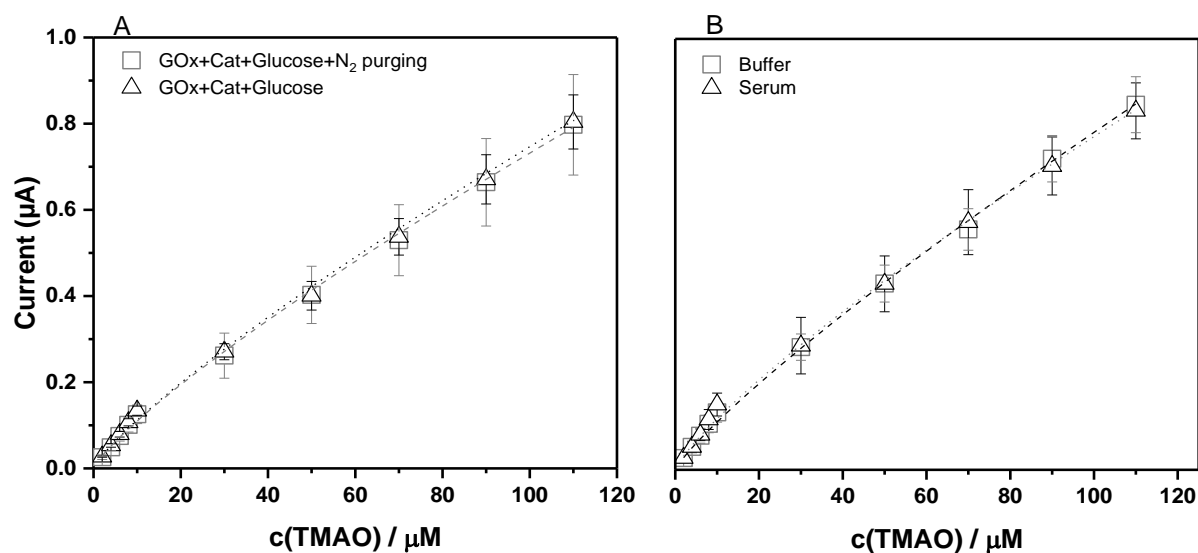


Figure 5. Graph of the current response versus the concentration of TMAO A) N₂ purging additional on the O₂ removal system (squares) and without purging (triangles). B) in undiluted serum (triangles) and in buffer solution (squares). Potassium phosphate buffer 100 mM pH 6.5; Range of TMAO 2-110 μM ; Methyl viologen 250 μM ; GOx 8 U, Cat 200 U and glucose 50 mM, (n=3 electrodes)

To validate the oxygen removal system and confirm our results, the same measurement was performed except that additional N₂ purging was applied before and during the measurement (Fig 5A, squares). Thus, the measuring buffer containing GOx, Cat and glucose was purged with N₂ prior to the measurement for 30 min and then gently flushed continuously over the liquid phase during the whole measurement cycle. It is clear from the graph depicting the current versus the applied TMAO concentration that there is no difference in the performance between the sensor responses and thus, the O₂ removal capacity of the system is optimal and no residual oxygen interferes during the measurements.

Further, we also tested the reproducibility and stability of the biosensor. No obvious decrease of response was noted after 20 repetitive measurements over a period of 6 hours. The relative standard deviation (RSD) for these measurements is 8.8 %. Between each measurement the measuring cell was washed thoroughly with the measuring buffer. The results (SI Fig 4) indicate that the biosensor is stable for prolonged measurements during one day. After storage of the biosensor in 75 mM Tris buffer (currently used for enzyme storage in solution) at 4 °C for one week, the signal response dropped only by $\approx 13 \%$ ($12.67 \pm 4 \%$; SI Fig 5). Since the

electrode is covered with a dialysis membrane which prevents leaching of the enzyme from the electrode surface, we ascribe this loss of the initial response to the enzyme inactivation.

3.5. Biosensor performance in serum

A potential application of the biosensor is the determination of TMAO in serum samples. Therefore, recovery of TMAO in serum was tested and also the effect of serum on the sensitivity of the TMAO biosensor. An important point for the performance of this biosensor is the very small influence of the serum on the signal produced from the catalysis of TMAO by the immobilized TMAO reductase. In a series of experiments, we tested this aspect by injecting diluted serum spiked with 20 μM TMAO. The response was only 7 % lower for the spiked human serum sample compared to the same concentration of TMAO in buffer solution (67 ± 0.5 nA vs. 72 ± 1 nA, respectively) (SI Fig 6). This indicates that there are no substances in serum that can significantly interfere during the detection of TMAO by the immobilized TorA-FDH which is highly specific for TMAO.

The next measurement was performed in undiluted serum containing additionally the O_2 removing system. After equilibration of the sensor the current generated upon consecutive additions of TMAO at different concentrations was evaluated. As can be seen from Fig 5b (black squares) the linearity and sensitivity in the range between 2-110 μM are nearly the same compared to measurement in pure buffer solution (red circles) where the sensitivity in buffer solution is 14.16 nA/ μM and in undiluted serum solution 13.75 nA/ μM TMAO. This shows that the biosensor can perform the measurements without any interferences or need for serum dilution for detecting the TMAO in a real time serum sample. Altogether these results indicate that the sensitivity is not markedly influenced when using real samples.

4. Conclusion

Here, we report on the development of the first enzyme-based TMAO biosensor involving a chimeric TMAO reductase from *E.coli*. Such design of recognition molecules represents a generic approach for new biosensors. Our results show that the biosensor made up with the chimeric enzyme has better characteristics than that with the wild type enzyme. The sensitivity and linear range of operation of the reported biosensor is in the desirable range for addressing the values of TMAO in blood of healthy people. The short-term usage stability is

quite good. The sensor can operate over prolonged daily measurements. The serum measurements show that a detection of TMAO in human serum can be performed without interferences from the complex serum matrix. Furthermore, the incorporated O₂ removal system, consisting of GOx and Cat allows for performing measurements under ambient air conditions without intervening in the detection of TMAO and even high negative potentials can be applied without the risk of having overlapping signals from the O₂ reduction. Given the increased abundance of data for the involvement of TMAO in humans as a potential biomarker for several disease states, a fast and simple sensor for TMAO detection is preferred.

Acknowledgment

The financial support by the Deutsche Forschungsgemeinschaft (DFG) for funding the Unicat cluster of excellence (EXC 314) is gratefully acknowledged. We would like to thank Kim Tiedemann for providing a sample of TorA-WT.

References

- Abo, M., Ogasawara, Y., Tanaka, Y., Okubo, A., Yamazaki, S., 2003. *Biosens. Bioelectron.* 18, 735–739.
- Aguey-Zinsou, K.-F., Bernhardt, P. V, McEwan, A.G., Ridge, J.P., 2002. *JBIC J. Biol. Inorg. Chem.* 7, 879–883.
- Bae, S., Ulrich, C.M., Neuhausser, M.L., Malysheva, O., Bailey, L.B., Xiao, L., Brown, E.C., Cushing-Haugen, K.L., Zheng, Y., Cheng, T.-Y.D., Miller, J.W., Green, R., Lane, D.S., Beresford, S.A.A., Caudill, M.A., 2014. *Cancer Res.* 74, 7442–52.
- Bell, J.D., Lee, J.A., Lee, H.A., Sadler, P.J., Wilkie, D.R., Woodham, R.H., 1991. *Biochim. Biophys. Acta - Mol. Basis Dis.* 1096, 101–107.
- Benesch, R.E., Benesch, R., 1953. *Science* 118, 447–448.
- Bennett, B.J., Vallim, T.Q. de A., Wang, Z., Shih, D.M., Meng, Y., Gregory, J., Allayee, H., Lee, R., Graham, M., Crooke, R., Edwards, P.A., Hazen, S.L., Lusis, A.J., 2013. *Cell Metab.* 17, 49–60.
- Buc, J., Santini, C.-L., Giordani, R., Czjzek, M., Wu, L.-F., Giordano, G., 1999. *Mol. Microbiol.* 32, 159–168.
- Cheng, H., Abo, M., Okubo, A., 2003. *Analyst* 128, 724–727.
- daCosta, K.-A., Vrbanac, J.J., Zeisel, S.H., 1990. *Anal. Biochem.* 187, 234–239.
- Englander, S.W., Calhoun, D.B., Englander, J.J., 1987. *Anal. Biochem.* 161, 300–306.

- Fennema, D., Phillips, I.R., Shephard, E.A., 2016. *Drug Metab. Dispos.* 44, 1839–1850.
- Fourmond, V., Baffert, C., Sybirna, K., Lautier, T., Abou Hamdan, A., Dementin, S., Soucaille, P., Meynial-Salles, I., Bottin, H., Léger, C., 2013. *J. Am. Chem. Soc.* 135, 3926–3938.
- Gamati, S., Luong, J.H.T., Mulchandani, A., 1991. *Biosens. Bioelectron.* 6, 125–131.
- Iobbi-Nivol, C., Pommier, J., Simala-Grant, J., Méjean, V., Giordano, G., 1996. *Biochim. Biophys. Acta - Protein Struct. Mol. Enzymol.* 1294, 77–82.
- Kaufmann, P., Duffus, B.R., Mitrova, B., Iobbi-Nivol, C., Teutloff, C., Nimtz, M., Jansch, L., Wollenberger, U., Leimkühler, S., 2018. *Biochemistry* 57, 1130–1143.
- Kühn, T., Rohrmann, S., Sookthai, D., Johnson, T., Katzke, V., Kaaks, R., von Eckardstein, A., Müller, D., 2017. *Clin. Chem. Lab. Med.* 55, 261–268.
- Mafra, D., Lobo, J.C., Barros, A.F., Koppe, L., Vaziri, N.D., Fouque, D., 2014. *Future Microbiol.* 9, 399–410.
- Mamer, O.A., Choinière, L., Lesimple, A., 2010. *Anal. Biochem.* 406, 80–82.
- Michaelis, L., Hill, E.S., 1933. *J. Gen. Physiol.* 16, 859–873.
- Nihon Seikagakkai. I., Okubo, N., Ishimoto, M., 1986. *J. Biochem.* 99, 1773–1779.
- Plumeré, N., Henig, J., Campbell, W.H., 2012. *Anal. Chem.* 84, 2141–2146.
- Schulz, C., Ludwig, R., Gorton, L., 2014. *Anal. Chem.* 86, 4256–4263.
- Smith, J.L., Wishnok, J.S., Deen, W.M., 1994. *Toxicol. Appl. Pharmacol.* 125, 296–308.
- Stubbs, J.R., House, J.A., Ocque, A.J., Zhang, S., Johnson, C., Kimber, C., Schmidt, K., Gupta, A., Wetmore, J.B., Nolin, T.D., Spertus, J.A., Yu, A.S., 2016. *J. Am. Soc. Nephrol.* 27, 305–13.
- Tavahodi, M., Ortiz, R., Schulz, C., Ekhtiari, A., Ludwig, R., Haghghi, B., Gorton, L., 2017. *Chempluschem* 82, 546–552.
- Velasquez, M., Ramezani, A., Manal, A., Raj, D., 2016. *Toxins (Basel)*. 8, 326–337.
- Wang, Z., Klipfell, E., Bennett, B.J., Koeth, R., Levison, B.S., Dugar, B., Feldstein, A.E., Britt, E.B., Fu, X., Chung, Y.M., Wu, Y., Schauer, P., Smith, J.D., Allayee, H., Tang, W.H.W., DiDonato, J.A., Lusis, A.J., Hazen, S.L., 2011. *Nature* 472, 57–65.
- Wang, Z., Levison, B.S., Hazen, J.E., Donahue, L., Li, X.-M., Hazen, S.L., 2014. *Anal. Biochem.* 455, 35–40.
- Zhu, W., Gregory, J.C., Org, E., Buffa, J.A., Gupta, N., Wang, Z., Li, L., Fu, X., Wu, Y., Mehrabian, M., Sartor, R.B., McIntyre, T.M., Silverstein, R.L., Tang, W.H.W., DiDonato, J.A., Brown, J.M., Lusis, A.J., Hazen, S.L., 2016. *Cell* 165, 111–124.
- Zu, Y., Shannon, R.J., Hirst, J., 2003. *J. Am. Chem. Soc.* 125, 6020–6021.

Supplementary Material

[Click here to download Supplementary Material: Mitrova Supporting Information.pdf](#)